Available online at www.sciencedirect.com

SciVerse ScienceDirect

Ceramics International 39 (2013) 1285–1292

CERAMICS INTERNATIONAL

www.elsevier.com/locate/ceramint

The PZT system ($PbTi_xZr_{1-x}O_3$, $0 \le x \le 1.0$): The real phase diagram of solid solutions (room temperature) (Part 2)

I.N. Andryushina*, L.A. Reznichenko, L.A. Shilkina, K.P. Andryushin, S.I. Dudkina

Research Institute of Physics, Southern Federal University, Rostov-on-Don, 344090, Russian Federation, Rostov-on-Don, Stachki ave, 194, Russia

Received 10 July 2012; received in revised form 11 July 2012; accepted 12 July 2012
Available online 25 July 2012

Abstract

The sequence of phase transformations in the ceramic system $PbTi_xZr_{1-x}O_3$ ($0 \le x \le 1.0$) is determined and the real phase diagram of solid solutions is built. The observed periodicity of phase formation processes in the rhombohedral and tetragonal regions is explained by the real (defective) structure of PZT system ceramics, which is in many respects related to the variable valence of Ti ions and, as a result, to formation, accumulation, and ordering of point defects (oxygen vacancies) and their elimination by crystallographic shifts. The obtained results are useful in interpretation of the macroscopic properties of ceramics based on the PZT system.

Keywords: D.PZT; Phase diagram; Room temperature; Point defects

1. Introduction

The binary system $PbZr_{1-x}Ti_xO_3$ (PZT) is an example of ferroelectric (FE) solid solutions (SS), which has high technological value and is widely used in piezoelectric material science and instrument-making industry. In a narrow compositional range centered at $x \sim 0.50$ the phase diagram contains the morphotropic region (MR) (the region of concentration rhombohedral (Rh)–monoclinic (M)–tetragonal (T) phase transitions), which makes this system of fundamental importance. The intervening (monoclinic) phases recently discovered in MR [1] determine high piezoelectric properties of the SS. Recently the scientific interest in this system resumed, but it was constrained to the study of selected chemical compositions. The systematic and detailed (with small concentration increments) study of the behavior of this SS in the whole solubility interval ($0.00 \le x \le 1.00$) under combined external influences was practically not conducted. Taking into account that to this day the PZT system remains unique and important, it appears essential to conduct studies aimed at establishment of the principles of the crystal structure formation in the indicated concentration range.

In [2] we have conducted a systematic study of PZT solid solutions in the range $0.37 \le x \le 0.57$. The x-T-(T=298 K) phase diagram of the system is built, which contains isosymmetrical states in single-phase regions, characterized by differing behavior of structural and electrophysical parameters, as well as regions of their coexistence with constant unit cell volumes. The explanation of appearance of such states was given in the framework of the real (defective) structure of objects. Several causes responsible for the appearance of phase states were pointed out, which are related to the peculiarities of solid solutions: variable valence of the titanium ions, extremely adaptive structure of its dioxide, formation, ordering and rotations of crystallographic shift planes. It is shown that the transition from the rhombohedral to the tetragonal phase occurs not directly, but through two intervening lower symmetry phases, whose appearance is favored by the defects developing in the solid solutions.

The aim of the present work is the determination of phase transitions sequence in $PbZr_{1-x}Ti_xO_3$ ($0 \le x \le 1.0$) ceramics and the construction of the real phase diagram of SS.

The objects under study, their synthesis and experimental methods are described in detail in [3].

*Corresponding author. Tel.: +78632434066.
E-mail addresses: futur6@mail.ru, vortexblow@gmail.com (I.N. Andryushina).

0272-8842/$ - see front matter
http://dx.doi.org/10.1016/j.ceramint.2012.07.060

2. Experimental results and discussion.

2.1. The region of rhombic (R)–rhombohedral (Rh) transition.

In the region adjacent to $PbZrO_3$ the resulting SS possess the same R symmetry as $PbZrO_3$ up to $x=0.065$ in contrast to the value $x=0.057$ reported earlier [4]. The morphotropic R–Rh transition occupies the concentration range $0.045 \le x \le 0.065$ (Fig. 1). Fig. 2 shows the change of the diffraction pattern during the transition. It can be seen from the figure that at $x=0.045$ the intensity at maximum abruptly declines and the width of the diffraction lines 240 and 004 increases, whereas the single line 042 (the indices are in rhombic setting) has pronounced anisotropy in the lower θ angles region, where under subsequent x increase appears a maximum corresponding to the (1 1 1) reflection of the Rh phase. The line 240 splits into two peaks, one of which is the diffraction reflection of the 240R phase, whereas the other is the 2 0 0 reflection of the Rh phase. The traces of the R phase reflections are still observed at $x=0.065$. The unit cell volume of the Rh phase is larger than that in the R phase by $\Delta V_{exp}=0.4$ Å^3 at $x=0.0525$ and $\Delta V_{exp}=0.55$ Å^3 at $x=0.0575$.

2.2. The rhombohedral region.

In the range $0.065 \le x \le 0.36$ SS possess Rh symmetry. Fig. 3 shows concentration dependence of the structural parameters and of the single 2 0 0 diffraction line half-width $B_{2\,0\,0}$. It can be seen that upon approaching the MR $B_{2\,0\,0}$ increases with the rise possessing periodic character. The angle α exhibits noticeable jumps at $x=0.14$ and 0.30. Table 1 comprises the experimental and theoretical unit

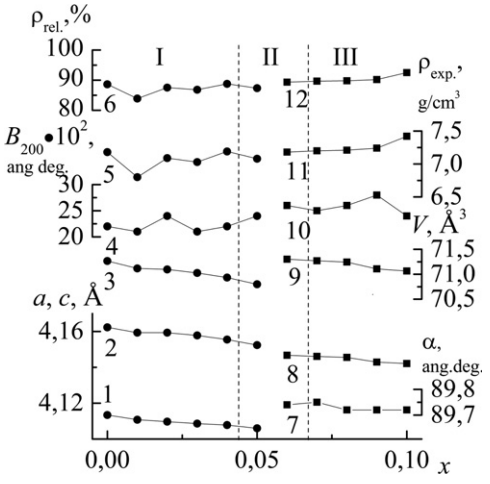

Fig. 1. Dependencies of structural parameters, half-width of the 2 0 0 diffraction line $B_{2\,0\,0}$, experimental $\rho_{exp.}$, and relative $\rho_{rel.}$ densities of solid solutions on x in the interval $0.0 \le x \le 0.1$. The numbers denote: pseudotetragonal R cell parameters c (1), a (2), cell volume V (3), $B_{2\,0\,0}$ (4), $\rho_{exp.}$ (5), $\rho_{rel.}$ (6), and Rh cell parameters a (7), α (8), cell volume, V (9), $B_{2\,0\,0}$ (10), ρ_{exp} (11), ρ_{rel} (12).

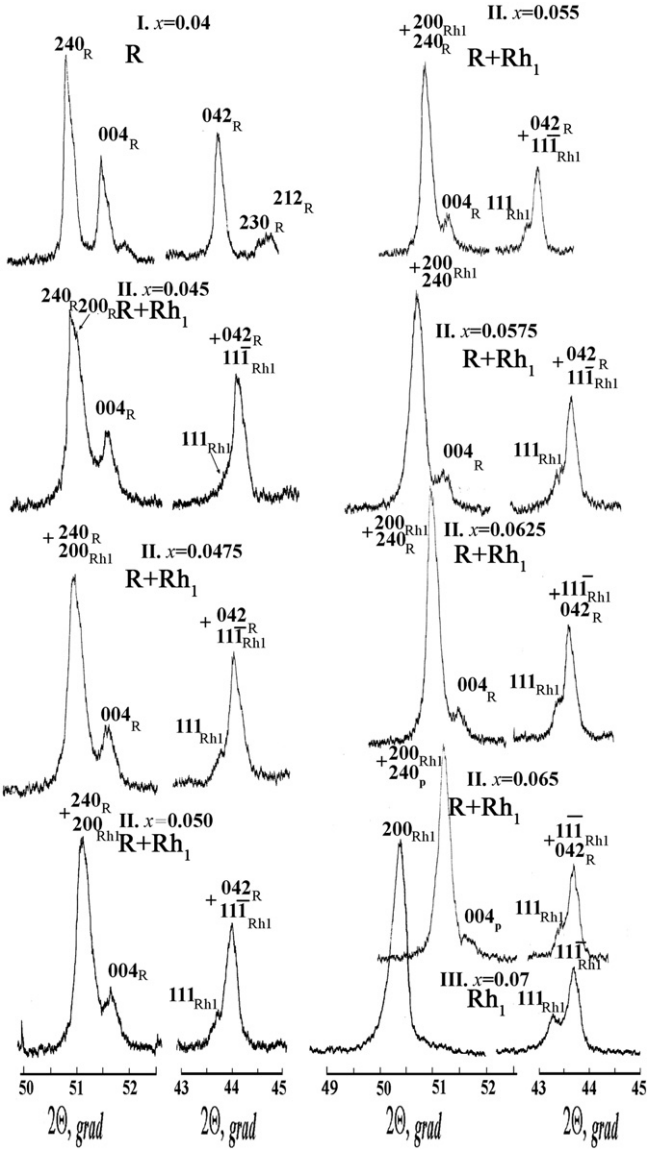

Fig. 2. Diffraction pattern fragments corresponding to various compositions of the $PbTi_xZr_{1-x}O_3$ SS from the region of R-Rh transition.

cell volumes and the rates of their decrease, $V'_{exp.}(x)$ and $V'_{teor}(x)$, with increase of x.

It is evident from the table that the decrease of V_{exp} with increasing x is nonuniform. At $x=0.09$, 0.11, 0.20, 0.24, 0.28, and 0.34 $V'_{exp.}(x)$ sharply decreases, whereas at $x=0.14$, 0.31, 0.35, and 0.36, on the contrary, increases as compared to $V'_{theor.}(x)$. The increase of $V'_{exp.}(x)$ is accompanied by the jumps of the parameter α. The decrease of $V'_{exp.}(x)$, i.e., the closeness to the invar effect (IE), evidences that in these concentration intervals lattice transformations occur. (The invar effects were revealed by us in the MR of the PZT system studied with concentration increments of $0.0025 \div 0.005$ [5]). The decrease of $V'_{exp.}(x)$ in the interval $0.09 \le x \le 0.10$ is most probably connected with disappearance of the R phase clusters, whereas in the interval $0.11 \le x \le 0.12$ with the nucleation of the new phase. Fig. 4 shows the diffraction line $(1\,1\,1)_c$

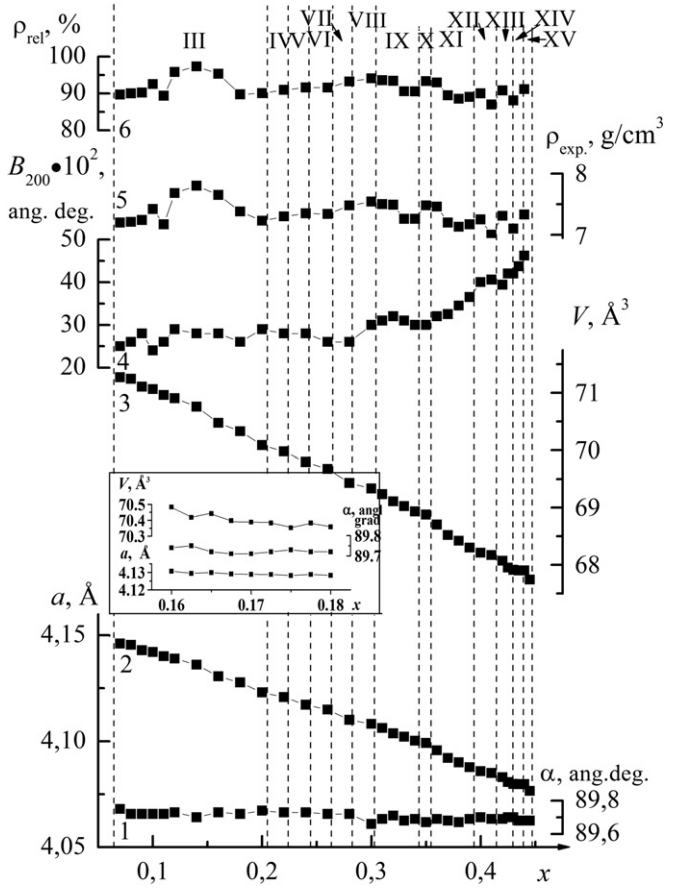

Fig. 3. Dependencies of structural parameters α (1) and a (2), cell volume V_{exp} (3), half-width of the 2 0 0 diffraction line $B_{2\,0\,0}$ (4), experimental ρ_{exp} (5), and relative $\rho_{rel.}$ (6) densities of SS on x in the interval $0.07 \le x \le 0.445$.

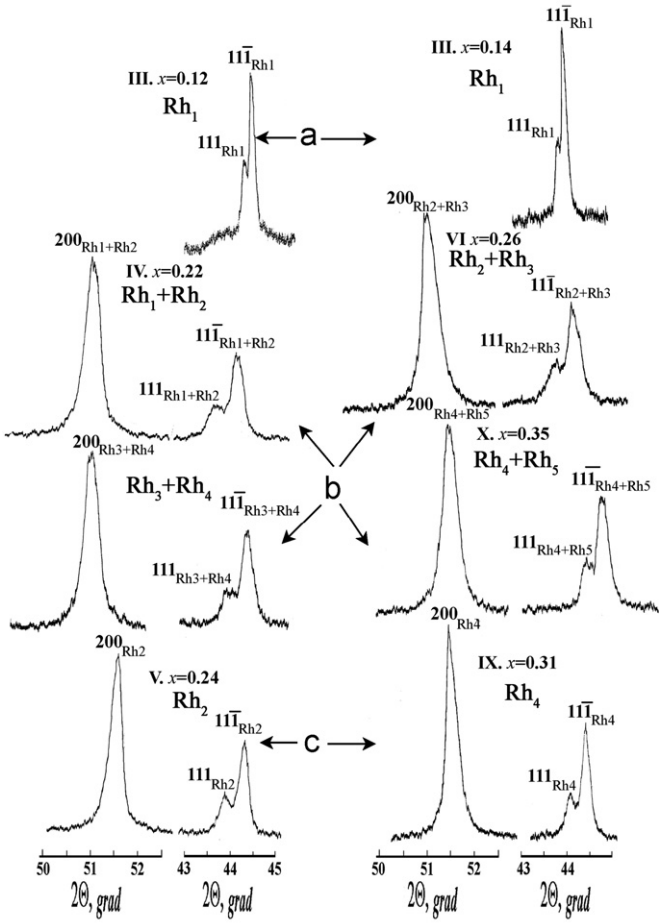

Fig. 4. Diffraction pattern fragments corresponding to various compositions of the $PbTi_xZr_{1-x}O_3$ SS from the Rh region.

Table 1
Experimental and theoretical cell volumes and their rates of change at increasing x (volume derivatives) in the rhombohedral phase.

x	V_{exp}, (Å^3)	$V'_{exp.}$ (x)	$V_{theor.}$, (Å^3)	$V'_{theor.}$ (x)
0.07	71.270	−7.25	73.888	−12.67
0.08	71.198	−9.03	73.762	−12.66
0.09	71.107	−4.19	73.635	−12.64
0.1	71.065	−10.29	73.509	−12.63
0.11	70.963	−5.76	73.382	−12.61
0.12	70.905	−7.37	73.256	−12.59
0.14	70.758	−14.10	73.004	−12.56
0.16	70.475	−7.40	72.753	−12.53
0.18	70.327	−12.04	72.502	−12.50
0.20	70.086	−5.56	72.252	−12.48
0.22	69.975	−9.14	72.003	−12.45
0.24	69.792	−5.85	71.754	−12.42
0.26	69.675	−12.24	71.505	−12.39
0.28	69.430	−4.78	71.258	−12.36
0.30	69.3348	−10.06	71.010	−12.34
0.31	69.2342	−13.99	70.887	−12.32
0.32	69.094	−6.89	70.764	−12.31
0.33	69.025	−9.23	70.641	−12.30
0.34	68.933	−5.4	70.518	−12.28
0.35	68.879	−17.58	70.395	−12.27
0.36	68.703	−17.83	70.272	−12.25

(in the pseudocubic setting) of the SS with $x=0.12$. It can be seen that the bottom of the line contains a halo, which is a sign of appearance of clusters of the new phase [6]. At this stage the new phase is represented by a packing of certain planes, which transform to a three-dimensional structure upon further increase of x.

In the interval $0.14 \le x \le 0.16$ V_{exp} decreases faster, than V_{theor}, i.e., a sharp structure compaction takes place. In [7,8] it is shown that the structure compaction in oxides containing ions with variable valence occurs along the crystallographic shift planes (CSP), with the exception of the (1 1 0) planes—the antiphase boundaries, which are found in the $PbZrO_3$ structure [9]. Thus one can argue that the new phase includes CSP's differing from the antiphase boundaries and, therefore, as shown in [5] possesses different symmetry. In favor of this assumptions is the jump of the rhombohedral angle α, as well as the drastic increase of the SS density with $x=0.12$, 0.14, 0.16 with its highest value at $x=0.14$ [3]. This is also in accordance with [10], where SS with $x=0.04$, 0.14, 0.23 were studied and a suggestion made that in the Rh phase there exist locally ordered regions with the symmetry differing from that of the average crystal structure. In [4] the authors also

distinguish solid solutions with $x=0.15$ and $x=0.36$. They have determined that in the range $0.15 \le x \le 1.0$ the phase transition line to the paraelectric phase on their phase diagram precisely coincides with that of Shirane [11], whereas at $0.0 < x \le 0.15$ deviates slightly. In the vicinity of $x=0.36$ the authors of [4] determine the transition between rhombohedral ferroelectric phases R3c and R3m.

Fig. 4b shows diffraction pattern fragments including the lines $(1\ 1\ 1)_c$ and 200 of SS with $x=0.22$, 0.26, 0.30, 0.35. The broadening of the lines and their splitting character points to the appearance of another phase with the same symmetry and close cell parameters. It means that the significant decrease of $V'_{exp.}(x)$ compared to $V'_{theor.}(x)$ (the proximity to the IE) in the ranges $0.20 < x \le 0.22$, $0.24 < x \le 0.26$, $0.28 < x \le 0.30$, and $0.34 < x \le 0.35$ is related to phase transformations. In order to confirm that the decrease of $V'_{exp.}$ is related to the invar effect we have obtained and studied solid solutions from the center of the single phase Rh region in the interval $0.16 < x \le 0.18$ with increments of $x=0.0025$ (at $x=0.16$ $V'_{exp.}=|7.4|$). The structural parameters are given in the inset of Fig. 3. It is evident from the figure that at $0.1675 \le x \le 0.1725$ the unit cell volume is constant, whereas the dependence of angle α on x experiences broad minimum. All this evidences of the processes occurring in the structure, which do not lead to the cell volume decrease, as it should be, when substituting an ion with a bigger radius (Zr) by a smaller one (Ti), but of the processes related, apparently, to oxygen octahedra rotations.

Fig. 4 (c) shows diffraction lines $(1\ 1\ 1)_c$ and 2 0 0 of SS with $x=0.24$, 0.31. Absence of peak splitting indicates that these SS are monophase. Thus, in the concentration ranges $0.18 < x \le 0.20$, $0.22 < x \le 0.24$, $0.26 < x \le 0.28$, and $0.30 < x \le 0.32$ the SS are monophase. In those concentration intervals where $V'_{exp.}$ is close to the theoretical value, the decrease of $V_{exp.}$ with increasing x occurs in accordance with diminution of the radius of the B cation. If $V'_{exp.}$ exceeds V'_{theor}, a new mechanism of the structure compaction emerges, related, from our point of view, to the size increase or to the rotation or appearance of new CSP.

It can be pointed out, that in paper [12], devoted to obtaining and study of $Pb(Ti_xZr_{1-x})O_3$ monocrystals, one observed that SS in the Rh phase possess far lower structural perfection as compared to the T phase crystals. The analysis [12] of the 2 0 0 reflection intensity distribution in the θ plane (2θ) showed the presence of separate maxima not related neither to the 71° twins, nor to the possible 180° domains off-orientation (this is very similar to the regions of co-existence of phase states). The maxima merge into one above the phase transition temperature from the ferroelectric to the paraelectric phase.

Therefore, the Rh region consists of five monophase regions ($0.065 < x \le 0.20$, $0.22 < x \le 0.24$, $0.26 < x \le 0.28$, $0.30 < x \le 0.34$, $0.35 < x \le 0.36$) and four regions of co-existence of phase states ($0.20 < x \le 0.22$, $0.24 < x \le 0.26$, $0.28 < x \le 0.30$, $0.34 < x \le 0.35$). The first broad monophase region includes the regions of structural changes occurring on the level of clusters.

The periodicity of the phase formation processes can be explained by the fact that upon the titanium (the ion with variable valence) concentration change, there occur formation, accumulation and ordering of oxygen vacancies, as well as their elimination by crystallographic shifts. The latter occurs at those x values when $V'_{exp.}(x)$ exceeds $V'_{teor.}(x)$, i.e., at $x=0.14$, 0.31, 0.35, 0.36. These SS are characterized by high experimental and relative densities [3]. The dispersion of SS densities in the Rh phase is related to the big number of restructurings in this concentration interval.

2.3. The tetragonal (T) region.

Fig. 5 shows concentration dependencies of the structural parameters a, c and V_{exp}, the distortion degrees of the T cell c/a-1, and half-widths $B_{1\,1\,1}$ of the single diffraction line 1 1 1. The change of $B_{1\,1\,1}$ with increasing x, similar to the Rh phase, has periodic character with the minimum value at $x=0.8$, where $V_{exp} \approx V_{theor}$.

Table 2 shows V_{exp}, V_{theor}, $V'_{exp.}(x)$, and $V'_{teor}(x)$. It is evident from the table that there are no such sharp

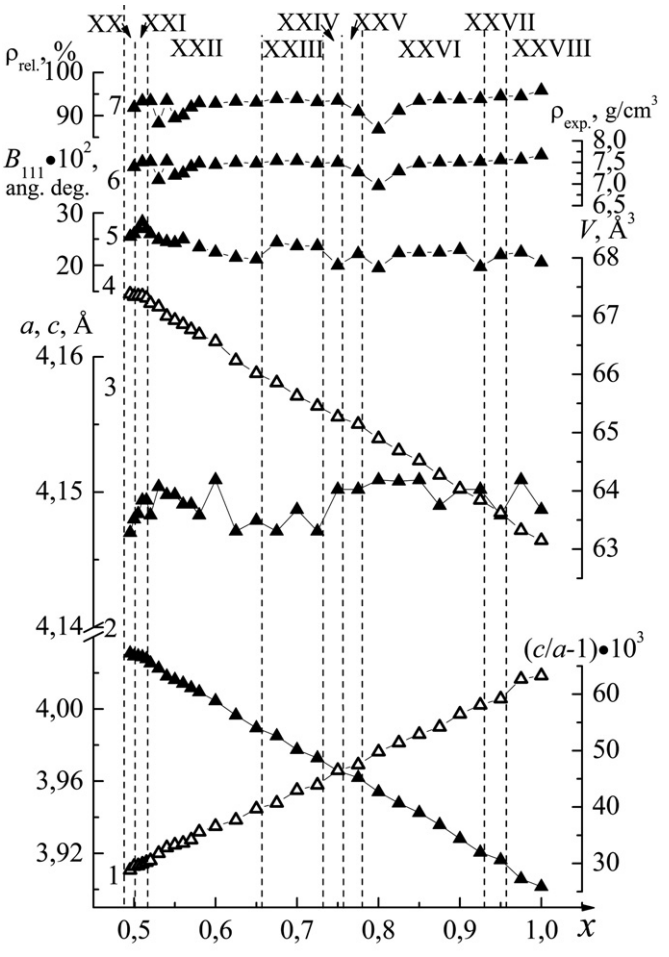

Fig. 5. Dependencies of structural parameters a (2), c (3), c/a-1 (1), V (4), half-width of the 1 1 1 diffraction line $B_{1\,1\,1}$ (5), experimental ρ_{exp} (6), and relative ρ_{rel} (7) densities of SS on x in the interval $0.495 \le x \le 1.0$.

Table 2
Experimental and theoretical cell volumes and their rates of change at increasing x (volume derivatives) in the tetragonal phase.

x	V_{exp}, (Å^3)	V'_{exp} (x)	V_{theor}, (Å^3)	V'_{theor} (x)
0.58	66.629	−3.27	67.609	−11.93
0.60	66.564	−13.09	67.371	−11.90
0.625	66.237	−8.74	67.073	−11.87
0.65	66.018	−6.43	66.776	−11.83
0.675	65.858	−9.08	66.480	−11.80
0.70	65.631	−6.99	66.185	−11.76
0.725	65.456	−7.45	65.891	−11.73
0.75	65.270	−4.95	65.598	−11.69
0.775	65.146	−9.92	65.306	−11.66
0.80	64.898	−8.24	65.014	−11.62
0.825	64.692	−6.92	64.724	−11.59
0.85	64.519	−9.86	64.434	−11.55
0.875	64.272	−9.38	64.145	−11.52
0.90	64.038	−7.84	63.857	−11.48
0.925	63.842	−8.54	63.570	−11.45
0.95	63.628	−12.16	63.284	−11.42
0.975	63.324	−6.95	62.998	−11.38
1.0	63.151		62.714	

oscillations of $V'_{exp.}(x)$ as in the Rh phase. Nevertheless one can expect phase state changes in the intervals $0.65 < x \leq 0.675$ ($V'_{exp.}(0.65) \approx 6$) and $0.75 < x \leq 0.775$ ($V'_{exp.}$ $(0.75) \approx 5$). The analysis of diffraction line profiles (Fig. 6a) showed that in these concentration intervals the SS are not monophase, the first of these intervals being broadened up to $x=0.725$. Furthermore, with x increase there appear signs of short range ordering—the wings of the lines possess asymmetric diffuse maxima (showed by arrows), whose intensity rises with x increase, whereas the width diminishes (Fig. 6b).

Such diffraction pattern is typical for structures possessing ordered plane defects [13], and the more precisely the order is obeyed the narrower the satellite diffuse maxima are. At $x=0.95$ the diffraction pattern sharply changes—the diffuse maxima width increases and the line 2 0 0 splits into three peaks (Fig. 6b), which evidences of the new structural change. Therefore, the periodicity of the phase formation processes exists in the T phase as well as in the Rh one. The monophase regions are situated in the intervals $0.58 \leq x \leq 0{,}65$, $0.725 < x \leq 0.75$, $0.775 < x \leq 0.925$, $0.95 < x \leq 1.0$, four regions altogether. Two-phase regions are located in the intervals $0.65 < x \leq 0.725$, $0.75 < x \leq 0.775$, $0.925 < x \leq 0.95$, three regions altogether.

The constancy of the c parameter at x change was pointed out earlier in [4,14], but the authors did not give any explanation to this phenomenon. We suggest the following interpretation. Upon crystallographic shifts giant elastic tensile stresses are developed in the defect region [7,8], in order for which to decrease the B cations and oxygens shift from their ideal positions along CSP (i.e., in the [0 0 1] direction upon distortion of the T cell), but in the opposite directions to the maximum possible for the given oxide distances [15]. Therefore introduction of the zirconium ions in the crystal structure with substantially bigger

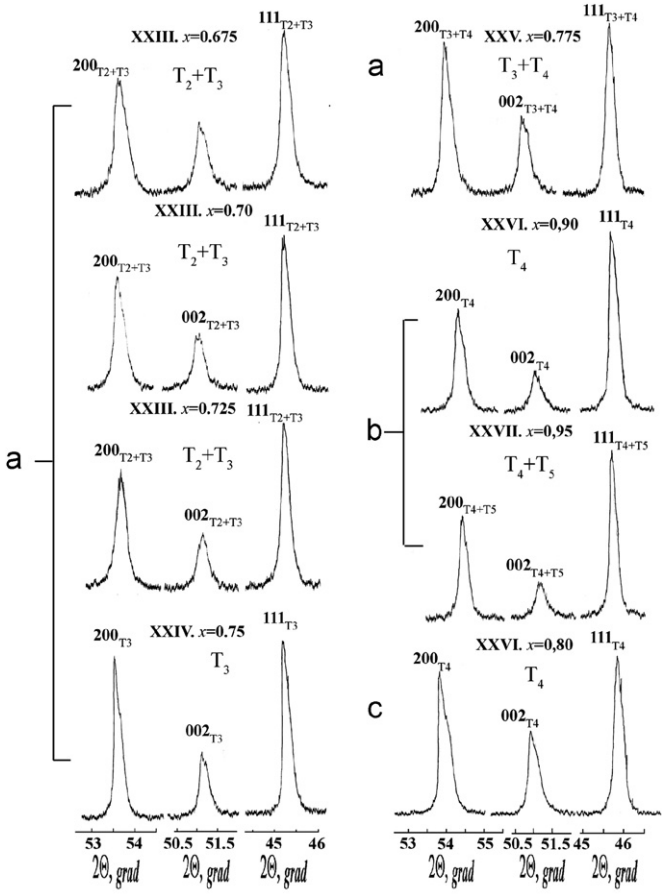

Fig. 6. Diffraction pattern fragments corresponding to various compositions of the $PbTi_xZr_{1-x}O_3$ SS from the T region.

radius, than that of titanium, cannot lead to the still larger shifts of atoms in the given direction and, thus, to the increase of the parameter c.

At the same time the parameter a in the T phase decreases much faster than in the Rh phase (the "concentration" expansion coefficient by analogy with the thermal expansion coefficient has the value in the Rh phase $(1/a_{Rh})\Delta a_{Rh}/\Delta x = -0.044$ and $(1/a_T)\Delta a_T/\Delta x = -0.063$ in the tetragonal phase). One should point out that for the tetragonal SS the external electric field application does not lead to the c parameter increase either [16,17].

SS with $x=0.80$ is particularly interesting. The relative density of this SS does not exceed 87%. Attempts to increase the density by changing sintering regimes did not give any results. At high sensitivity of the cell parameters to the preparation conditions this SS is remarkable for its structural stability. Fig. 6c gives the diffraction line profiles 1 1 1, 0 0 2 and 2 0 0 of this SS. One can see that they differ from the corresponding lines of other SS, whose diffraction patterns were obtained under the same conditions, by higher intensity, smaller width and minor smearing in the region of the wings, which evidences of a high structural perfection of SS with this composition. The equality of V_{exp} and V_{theor} is reached at $x=0.83$, but one should take

into account that V_{theor} is calculated for the chemical formula $A(B'_xB''_{1-x})O_3$ neglecting the fact that in essence $PbTiO_3$ is the inner solid solution or an autoisomorphous substance [18], whose formula has the form

$$Pb_{1-x}[Ti_{1-(x_2+x_3)}Pb^{4+}_{x_2}Pb^{2+}_{x3}]O_{3-y},$$

where $x=x_1+x_2+x_3$, x_1 is the PbO loss as a result of evaporation due to volatility, x_2 is the fraction of Pb^{4+} incorporated in the B-sublattice as a result of Pb^{2+} oxidation, x_3 is the fraction of Pb^{2+} incorporated in the B-sublattice owing to the CSP presence in the lattice. Therefore, one can assume that the SS with $x=0.80$ is the least defective and that the atomic displacements from the ideal positions are minimal. This is also confirmed by the fact that according to [19] upon decreasing x the E(1TO) soft mode frequency in the interval $1>x>0.75$ declines to vanishing values with a greater rate than at the temperature induced ferroelectric phase transition. Therefore, based on the obtained results of periodic changes upon x increase of the cell volume, half-width of the diffraction lines, density of the solid solutions, and the phase state, as well as lesser decrease rate of V_{exp} compared to V_{theor} due to the big number of invar effects, one can make the following conclusion. The reason for all these phenomena is the change in the real defective structure of solid solutions, namely the appearance, accumulation and ordering of the oxygen vacancies and their elimination by crystallographic shifts with the formation of crystallographic shift planes.

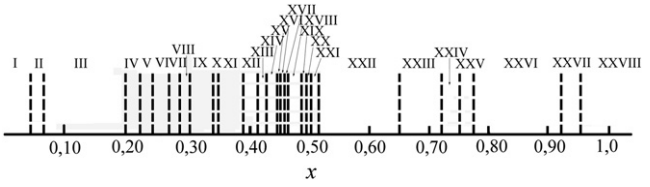

Fig. 7. x-T phase diagram of the real SS of the $PbZr_{1-x}TixO_3$ system in the concentration interval $0.0 \le x \le 1.0$ (isothermal cross-section at $T=298$ K). The notation of phases and phase states is given in Table 3.

The performed study allows drawing another conclusion important from the practical standpoint. The density of the ceramic samples of the solid solutions of this system depends not only on the sintering conditions, but also on their real structure. In some cases high density is achieved by conventional methods (e.g., for SS with x close to 0.14),

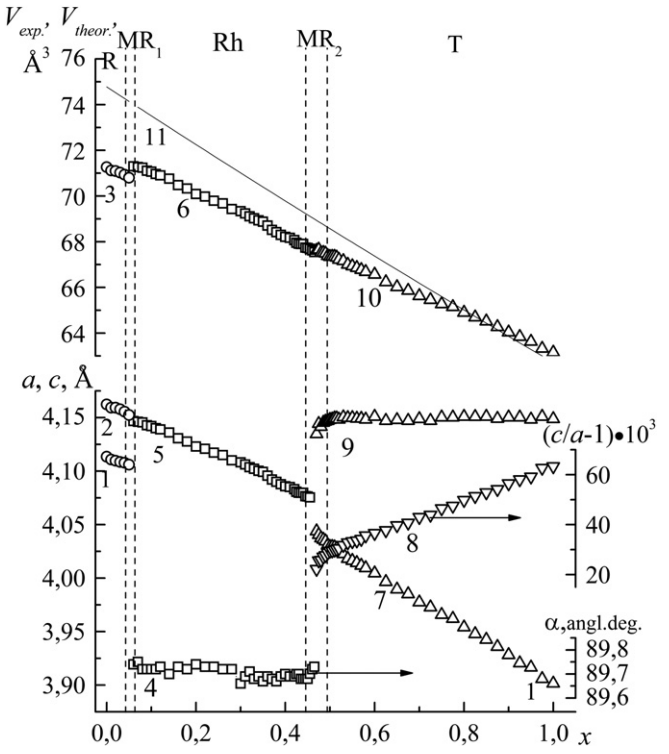

Fig. 8. Dependencies of structural characteristics of SS on x in the interval $0.0 \le x \le 1.0$: pseudotetragonal parameters of the R cell c (1) and a (2) and the cell volume V_{exp} (3), parameters of Rh cell α (4) and a (5) and the cell volume V_{exp} (6), parameters of the T cell a (7), c (9), and c/a-1 (8) and the cell volume V_{exp} (10), theoretical volume V_{theor} (11). The dotted lines show regions of MPT: MR_1 – the region of transition between the R and Rh phases, MR_2 – the region of transition between the Rh and T phases.

Table 3
Localization of phases, phase states and their coexistence regions of the PZT system for the concentration interval $0.0 \le x \le 1.0$.

Regions	Phase composition	Concentration interval	Regions	Symmetry	Concentration interval
I	R	$0 \le x \le 0.04$	XV	Rh_7	$0.44 < x \le 0.445$
II	$R+Rh_1$	$0.04 < x \le 0.065$	XVI	Rh_7+PSC_1	$0.445 < x \le 0.45$
III	Rh_1	$0.065 < x \le 0.20$	XVII	$Rh_7+PSC_1+PSC_2$	$0.45 < x \le 0.455$
IV	Rh_1+Rh_2	$0.20 < x \le 0.22$	XVIII	$Rh_7+PSC_1+PSC_2+T_1$	$0.455 < x \le 0.48$
V	Rh_2	$0.22 < x \le 0.24$	XIX	PSC_2+T_1	$0.48 < x \le 0.49$
VI	Rh_2+Rh_3	$0.24 < x \le 0.26$	XX	T_1	$0.49 < x \le 0.50$
VII	Rh_3	$0.26 < x \le 0.28$	XXI	T_1+T_2	$0.50 < x \le 0.515$
VIII	Rh_3+Rh_4	$0.28 < x \le 0.30$	XXII	T_2	$0.515 < x \le 0.65$
IX	Rh_4	$0.30 < x \le 0.34$	XXIII	T_2+T_3	$0.65 < x \le 0.725$
X	Rh_4+Rh_5	$0.34 < x \le 0.35$	XXIV	T_3	$0.725 < x \le 0.75$
XI	Rh_5	$0.35 < x \le 0.39$	XXV	T_3+T_4	$0.75 < x \le 0.775$
XII	Rh_5+Rh_6	$0.39 < x \le 0.41$	XXVI	T_4	$0.775 < x \le 0.925$
XIII	Rh_6	$0.41 < x \le 0.425$	XXVII	T_4+T_5	$0.925 < x \le 0.95$
XIV	Rh_6+Rh_7	$0.425 < x \le 0.44$	XXVIII	T_5	$0.95 < x \le 1.0$

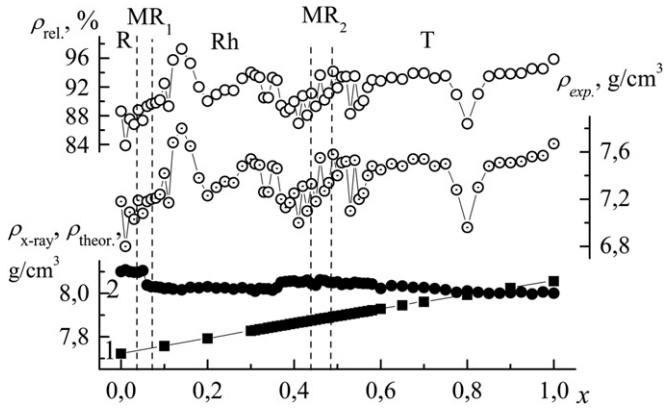

Fig. 9. Densities of SS in the interval $0.0 \le x \le 1.0$: theoretical ρ_{theor} (1), X-ray $\rho_{x\text{-}ray}$ (2), experimental ρ_{exp} (3), and relative ρ_{rel} (4).

whereas in other cases even the use of special methods does not lead to obtaining of high density ceramics (e.g., SS with x close to 0.80).

In the Rh phase the tricritical point is located at $x=0.06$ according to [20,21], at $x=0.10$ according to [22] and at $x=0.22$ according to [4]. In the T phase the second tricritical point is located at $x=0.72$ according to [23], at $x=0.55$ according to [4] and in the interval $0.6 \le x \le 0.7$ according to [14]. In [4] the transition between rhombohedral ferroelectric phases R3m and R3c is observed in the vicinity of $x=0.36$. Evidently the data dispersion is high and contains all the x values studied by us. In [24] it is stated that local displacements of lower symmetry are present in the tetragonal region, which is reflected in the diffraction peaks broadening (see also Refs. [25,26] in [24]). As a result of the study the phase diagram is built, which is shown in Fig. 7. The localization of phases, phase states and of their coexistence regions is given in Table 3.

Fig. 8 presents the overall picture of concentration changes of the linear a, c and angle α parameters, the experimental V_{exp} and theoretical V_{theor} cell volumes, and the distortion degree of the T cell c/a-1 of the solid solutions (at room temperature). Dotted lines show the regions of morphotropic phase transitions (MPT). The theoretical volume is calculated according to the formula [27]

$$V_{teor.} = \left\{ \frac{n_{Pb}\sqrt{2}PbO + 2[n_{Ti}xL_{TiO} + n_{Zr}(1-x)L_{ZrO}]}{6} \right\}^3,$$

where L is the unstrained cation–oxygen bond length taking into account the oxygen coordination number and n is the cation valence.

The following features of the behavior of structural characteristics can be pointed out: with increasing x the experimental volume decreases slowly than the theoretical one and at $x=0.83$ their values become equal, the c parameter in the T phase remains constant in the whole concentration interval of existence of this phase, and the angle parameter α in the Rh phase is also nearly constant.

Fig. 9 shows the x dependencies of the sample densities: experimental ρ_{exp}, X-ray, $\rho_{x\text{-}ray}$, relative, ρ_{rel} and theoretical ρ_{theor}. The densities $\rho_{x\text{-}ray}$ and ρ_{theor} are calculated according to the formula $1.67\,M/V$ using V_{exp} and V_{theor}, respectively (M is the molecular weight of one cell). It can be seen that the experimental densities tend to increase as well as the theoretical ones, but with a very big dispersion in the rhombohedral phase. The maximum values of ρ_{exp} and ρ_{rel} are achieved at $x=0.14$, whereas the minimal at $x=0.8$.

3. Conclusions

1. It is determined that at room temperature:
   - the Rh region consists of five monophase regions ($0.065 < x \le 0.20$, $0.22 < x \le 0.24$, $0.26 < x \le 0.28$, $0.30 < x \le 0.34$, $0{,}35 < x \le 0.36$) and of four regions of phase state coexistence ($0.20 < x \le 0.22$, $0.24 < x \le 0.26$, $0.28 < x \le 0.30$, $0.34 < x \le 0.35$); at the same time the first broad monophase region includes regions of structural changes occurring at the cluster level;
   - the T region consists of four monophase regions ($0.58 \le x \le 0.65$, $0.725 \le x \le 0.75$, $0.775 \le x \le 0.925$, $0.905 \le x \le 1.0$) and of three regions of phase state coexistence ($0.65 < x \le 0.725$, $0.75 < x \le 0.775$, $0.925 < x \le 0.95$); at that the SS with $x=0.83$ is remarkable for the highest structure stability.
2. The observed periodicity of the phase formation processes in the Rh and T regions results from the real (defective) structure of SS ceramics of the PZT system; in many respects it is related to the variable valence of Ti ions and, as a consequence, with formation, accumulation and ordering of point defects (oxygen vacancies) and their elimination by crystallographic shifts.

The obtained results are expedient to use when interpreting the peculiarities of the formation of macroscopic properties of ceramics based on the PZT system.

Acknowledgements

We appreciate the help of Nikita Ter-Oganessian with the preparation of the manuscript.

This work was financially supported by the Ministry of Education and Science of the Russian Federation, State contract 16.513.11.3032.

References

[1] B. Noheda, Structure and high-piezoelectricity in lead oxide solid solutions, Current Opinion in Solid State & Materials Science 6 (2002) 27–34.

[2] L.A. Reznichenko, L.A. Shilkina, O.N. Razumovskaya, E.A. Yaroslavtseva, S.I. Dudkina, O.A. Demchenko, U.I. Urasov, A.A. Esis, I.N. Andrushina, Phase formation in near-morphotropic region of the $PbZr_{1-x}Ti_xO_3$ system, structural defects, and electromechanical properties of the solid solutions, Physics of the Solid State 51 (5) (2009) 1010–1018.

[3] I.N. Andryushina, L.A. Reznichenko, V.A. Alyoshin, L.A. Shilkina, et al., The PZT system ($PbZr_{1-x}Ti_xO_3$, $0.0 \le x \le 1.0$): specific features of recrystallization sintering and microstructures of solid solutions (Part 1, Ceramics International (2012).

[4] V.V. Eremkin, V.G. Smotrakov, E.G. Fesenko, Structural phase transitions in $PbZr_{1-x}Ti_xO_3$ crystals, Ferroelectrics 110 (1990) 137–144.
[5] O.A. Demchenko, Fazi, fazovie sostoiania i morfotropnie oblasti v n-komponentnih sistemah segnetoelektricheskih tverdih rastvorah. Avtoreferat diserrtacii… k.f.-m. n. Rostov-na-Donu, Rostovskii gosudarstvennii universitet, 2006 25 (in Russian).
[6] S.V. Titov, L.A. Shilkina, L.A. Reznichenko, S.I. Dudkina, O.N. Razumovskaya, S.I. Shevtsova, E.M. Kuznetsova, Structure clusterization preceding concentration phase transitions, Technical Physics Letters 26 (9) (2000) 810–813.
[7] U.D. Tretiakov, Himiya Nestehiometricheskih Okislov, Izdatelstvo Moskovskogo gosudarstvennogo universiteta, Moscow, 1974 364 (in Russian).
[8] A.G. Petrenko, V.V. Prisedskii, Defecti Structuri v Segnetoelektrikah, Uchebno- metodichkii kabinet po visshmu obrazovaniu pri Minvuze USSR, 1989 102 (in Russian).
[9] A.A. Dobrikov, O.V. Presnyakova, Planar defects in $PbZrO_3$ and $PbTiO_3$ single crystals. [Ploskie defekty v monokristallakh $PbZrO_3$ i $PbTiO_3$], Neorganiceskie materialy 17 (12) (1981) 2239–2242 In Russian.
[10] B. Noheda, A. Gonzalo, M. Hagen, Pulsed neutron diffraction study of Zr-rich PZT, Journal of Physics: Condensed Matter 11 (1999) 3959–3965.
[11] G. Shirane, K. Suzuki, A. Takeda, Phase transitions in solid solutions $PbZrO_3$ and $PbTiO_3$: II X-ray study, Journal of the Physical Society of Japan 7 (1952) 12–18.
[12] V.V. Eremkin, V.G. Smotrakov, E.S. Tsikhotskii, V.A. Aleshin, E.G. Fesenko, Preparation of crystals of $PbZr_{1-x}Ti_xO_3$ and investigation of their perfection, Izv. Akad. Nauk SSSR, Neorg. Mater. 23 (2) (1987) 284–287.
[13] A. Ginie, Rentgenografiya kristallov, Fiz.-mat.- lit. Moscow (1961) 604 (in Russia).
[14] G.A. Rossetti Jr., A. Navrotsky, Calorimetric investigation of tricritical behavior in tetragonal $Pb(Zr_xTi_{1-x})O_3$, Journal of Solid State Chemistry 144 (1999) 188–194.
[15] L.A. Reznichenko, L.A. Shilkina, S.V. Titov, O.N. Razumovskaya, Magnéli phases in Ti-containing oxides and their solid solutions, Crystallography Reports 48 (3) (2003) 377–383.
[16] B. Noheda, J.A. Gonzalo, R. Guo, S-E. Park, L.E. Cross, D.E. Cox, G. Shirane. The monoclinic phase in PZT: new light on morphotropic phase boundaries. Physics of Ferroelectrics. (AIP Conference Proceedings, vol. 535). Ed. by R. Cohen. 535 (2000) 304–313.
[17] R. Guo, L.E. Cross, S.E. Park, B. Noheda, D.E. Cox, G. Shirane, Origin of the high piezoelectric response in $PhZr_{1-x}Ti_xO_3$, Physical Review Letters 84 (2000) 5423–5426.
[18] S.V. Titov, L.A. Shilkina, O.N. Razumovskaya, L.A. Reznichenko, V.G. Vlasenko, A.G. Shuvaev, S.I. Dudkina, A.N. Klevtsov, Crystal chemistry of lead titanate in relation to its electrical properties, Inorganic Materials 37 (7) (2001) 718–725.
[19] G. Burns, S.A. Bruce, Raman spectra of polycrystalline solids; application to the $PbTi_{1-x}Zr_xO_3$ system, Physical Review Letters 25 (17) (1970) 1191–1194.
[20] R.W. Whatmore, R. Clarke, A.M. Glazer, Tricritical behaviour in $PbZr_xTi_{1-x}O_3$ solid solutions, Journal of Physics C: Solid State Physics 11 (1978) 3089–3312.
[21] K. Roleder, J. Haderek., Tricritical point in $PbZr_xTi_{1-x}O_3$ solid solutions, Phase Transitions 2 (4) (1982) 285–292.
[22] M.J. Haun, E. Furman, H.A. McKinstry, L.E. Cross, Thermodynamic theory of the lead zirconate-titanate solid solution system, Part II, Tricritical Behavior Ferroelectrics 99 (1989) 27–44.
[23] A. Amin, R.E. Newnham, L.E. Cross, Polarization levels, and Curie temperatures in ferroelectric $PbZrO_3$:$PbTiO_3$ solid solutions, Materials Research Bulletin 15 (1980) 721–728.
[24] D.E. Cox, B. Noheda, G. Shirane, Low temperature phase in $PbZr_{0,52}Ti_{0,48}O_3$: a nutron powder diffraction study, Physical Review B: Condensed Matter 71 (2005) 134110.
[25] A.Ya. Dantciger, O.N. Razumovskaya, L.A. Reznichenko, V.P. Sakhnenko, A.N. Klevtsov, S.I. Dudkina, L.A. Shilkina, N.V. Dergunova, A.N. Ribyanec, Mnogokomponentnie sistemi segnetoelektricheskih slozhnih oksidov: fizika, kristallohiya. Aspecti dizaina. segnetopiezoelektricheskih materialov. Izdatelstvo RGU, Rostov-na-Donu. 1, 2 (2001) 408, 365 (in Russian).
[26] V. Tennery, High-temperature phase transitions in $PbZrO_3$, Journal of the American Ceramic Society 49 (1966) 483–486.
[27] N.V. Dergunova, V.P. Sakhnenko, E.G. Fesenko, Raschet parametrov kristallicheskoi reshotki tverdih rastvorov okislov so strukturoi perovskita, Kristallographiya 23 (1) (1978) 94–98 (in Russian).